Nonlinear saturation of Weibel-type instabilities

Srinivasan B.,[1] Cagas P.,[1] Hakim A.,[2] and Scales W.[1]

[1]Virginia Tech, Blacksburg, VA, USA, [2]Princeton Plasma Physics Laboratory, Princeton, NJ, USA

VIRGINIA TECH

Introduction

Weibel-type instabilities (WI), which grow in plasmas with anisotropic velocity distribution, have been studied for many years and drawn recent interest due to their broad applicability spanning from laboratory laser plasmas to origins of intergalactic magnetic fields in astrophysical plasmas. Magnetic particle trapping has been considered the main mechanism of the nonlinear saturation of these instabilities.

Novel continuum kinetic simulations provide consistent results indicating magnetic trapping. However, these simulations additionally show the significant role of electrostatic trapping in cold counter-streaming beams. This electrostatic trapping works together with magnetic trapping and alters the saturation. The role of the electrostatic field is negligible when the populations are at higher temperatures.

Results presented in this work have been submitted for review [Cagas et al., 2017].

Numerical Model

This work uses the discontinuous Galerkin (DG) [Cockburn and Shu, 2001] discretization of the full non-relativistic Vlasov-Maxwell system implemented in the `Gkeyll` framework [Juno et al., 2017]. This approach involves directly discretizing the Vlasov equation for each species s

$$\frac{\partial f_s}{\partial t} + \mathbf{v}\cdot\frac{\partial f_s}{\partial \mathbf{x}} + \frac{q_s}{m_s}\left(\mathbf{E}+\mathbf{v}\times\mathbf{B}\right)\frac{\partial f_s}{\partial \mathbf{v}} = 0, \qquad (1)$$

where f is the particle distribution defined in phase-space. The species are then coupled together using the full Maxwell equations.

- Unlike the fluid methods, which are derived by taking the moments of Eq. (1), the continuum kinetic method does not make any assumptions about the shape of the particle distribution function.
- Since the full continuous distribution function is discretized, the results are not affected by statistical noise.
- Phase-space has high dimensionality (up to 6D) and needs to be discretized directly.

Growth Mechanism & Linear Theory

The WI growth mechanism can be explained on a case with two counter-streaming electron populations. Without any perturbation the system is in unstable equilibrium. However, any perturbation causes net currents to appear which in turn increase magnetic field perpendicular to the flow. The magnetic field then increases the filamentation. This positive feedback loop is causes the exponential growth of the magnetic field.

In a special case when the flows are in the y-direction and magnetic perturbation is purely in the z-direction as a function of x, only B_z develops and the full process can be described with just three phase space coordinates – x, v_x, and v_y.

In order to obtain the kinetic dispersion relation, the Vlasov equation (Eq. 1) is linearized and combined with the linearized Ampere's law. This then leads to the following kinetic dispersion relation,

$$\frac{1}{2} = \frac{\omega_0^2}{c^2k^2}\left[\zeta Z(\zeta)\left(1+\frac{u_d^2}{v_{th}^2}\right)+\frac{u_d^2}{v_{th}^2}\right]+\frac{v_{th}^2}{c^2}\zeta^2, \qquad (2)$$

where ω_0 is the plasma oscillation frequency, c is the speed of light, k is the instability wave-number, u_d is the drift speed of each population (assuming symmetric drift velocities u_d with respect to zero), and v_{th} is thermal speed. $\zeta = \omega/(\sqrt{2}v_{th}k)$, where $\omega = \omega_r + i\gamma$. $Z(\zeta)$ is the plasma dispersion function defined as

$$Z(\zeta) = \frac{1}{\sqrt{\pi}}\int_{-\infty}^{\infty}\frac{e^{-x^2}}{x-\zeta}\mathrm{d}x. \qquad (3)$$

Numerical Simulations

Two sets of simulations were performed; both use the same drift velocity and initial perturbation, but differ in the temperature.

	u_d/c	v_{th}/c	$k_0\lambda_D$
High-temperature beams	±0.3	0.3	0.04
Low-temperature beams	±0.3	0.031	0.04

With $u_d = v_{th}$, the two electron populations overlap and form one population with anisotropic temperature.

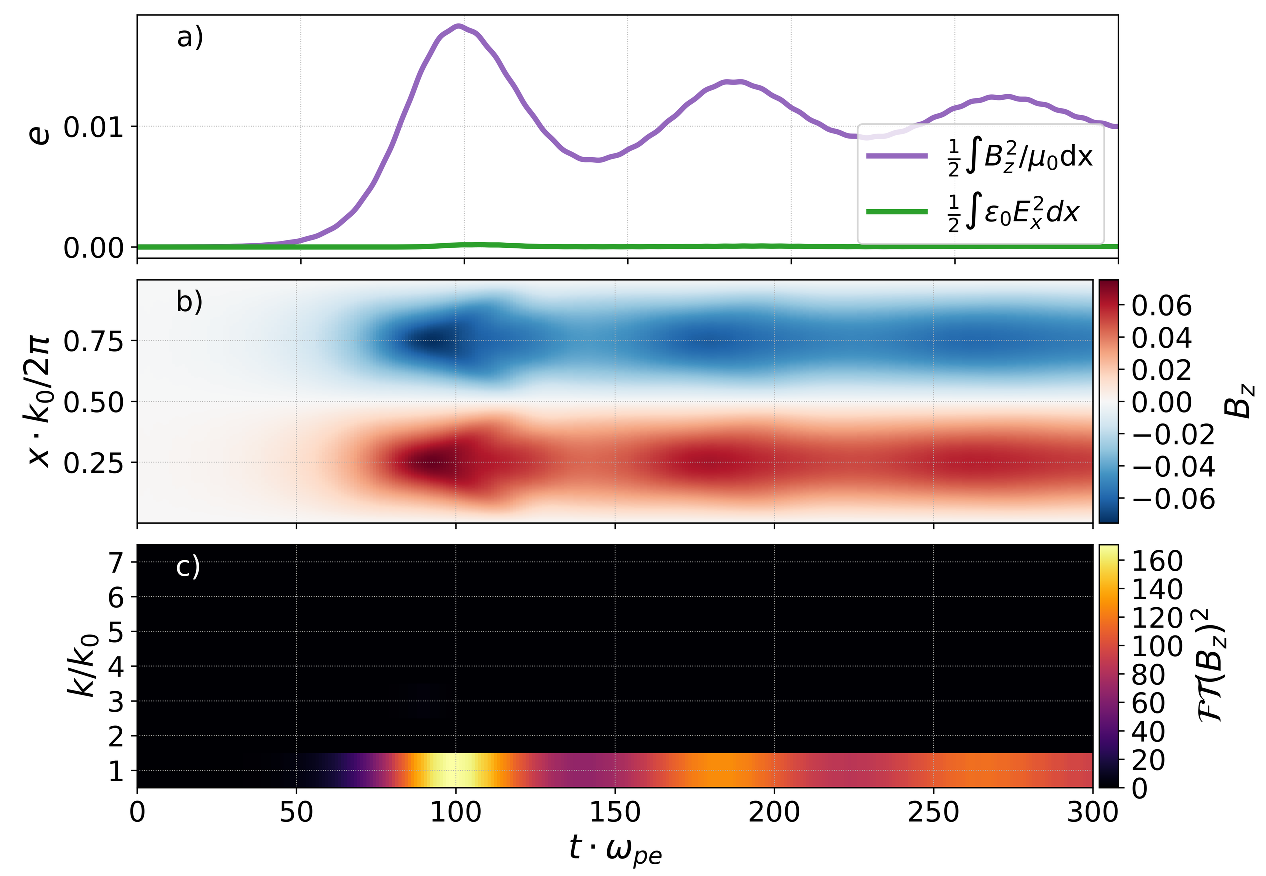

Figure 1: Evolution of the magnetic and electric field energies and magnetic field profiles for the high-temperature case.

The bounce period from the simulation

$$\frac{\omega_{sim}}{\omega_{pe}} \approx \frac{2\pi}{82} = 0.076,$$

corresponds very well to the theoretical magnetic bounce period [Davidson et al., 1972]

$$\frac{\omega_{theor}}{\omega_{pe}} = \sqrt{k\frac{q}{m}u_yB_z} \approx 0.077. \qquad (4)$$

The low-temperature case with two distinct electron beams, however, behaves differently. There is another frequency superimposed over the magnetic bounce frequency and the electric field grows considerably.

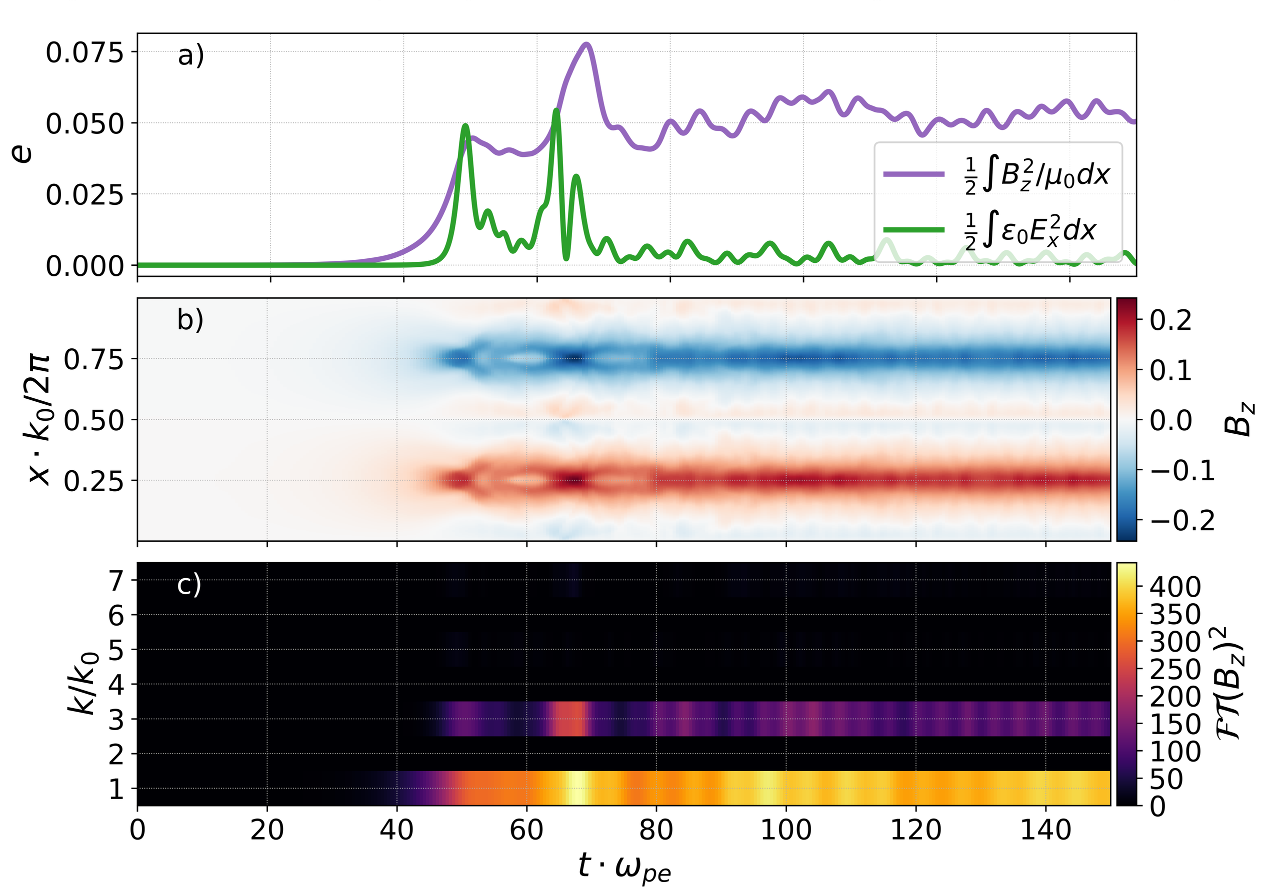

Figure 2: Evolution of the magnetic and electric field energies and magnetic field profiles for the low-temperature case.

Low-temperature Case

The transverse flows introduced by the magnetic field coupled with the nonuniform densities of the populations ($n^+(x) \neq n^-(x)$) are the main source of the electric field. Since $B_y = B_x = 0$ and $\partial B_z/\partial y = 0$, Ampere's law in the x-direction reduces to

$$\varepsilon_0\frac{\partial E_x}{\partial t} = -j_x = e\left[n^+u_x^+ + n^-u_x^-\right], \qquad (5)$$

where $\pm$ refers to the two counter-streaming electron populations.

The following figure shows the field variables and plasma variables for one population. In the region of magnetic field extremes (boundary between the populations forms here), the electric field increases to level that is comparable with the magnetic field. This electric field then quickly stops the filamentation flow in v_x.

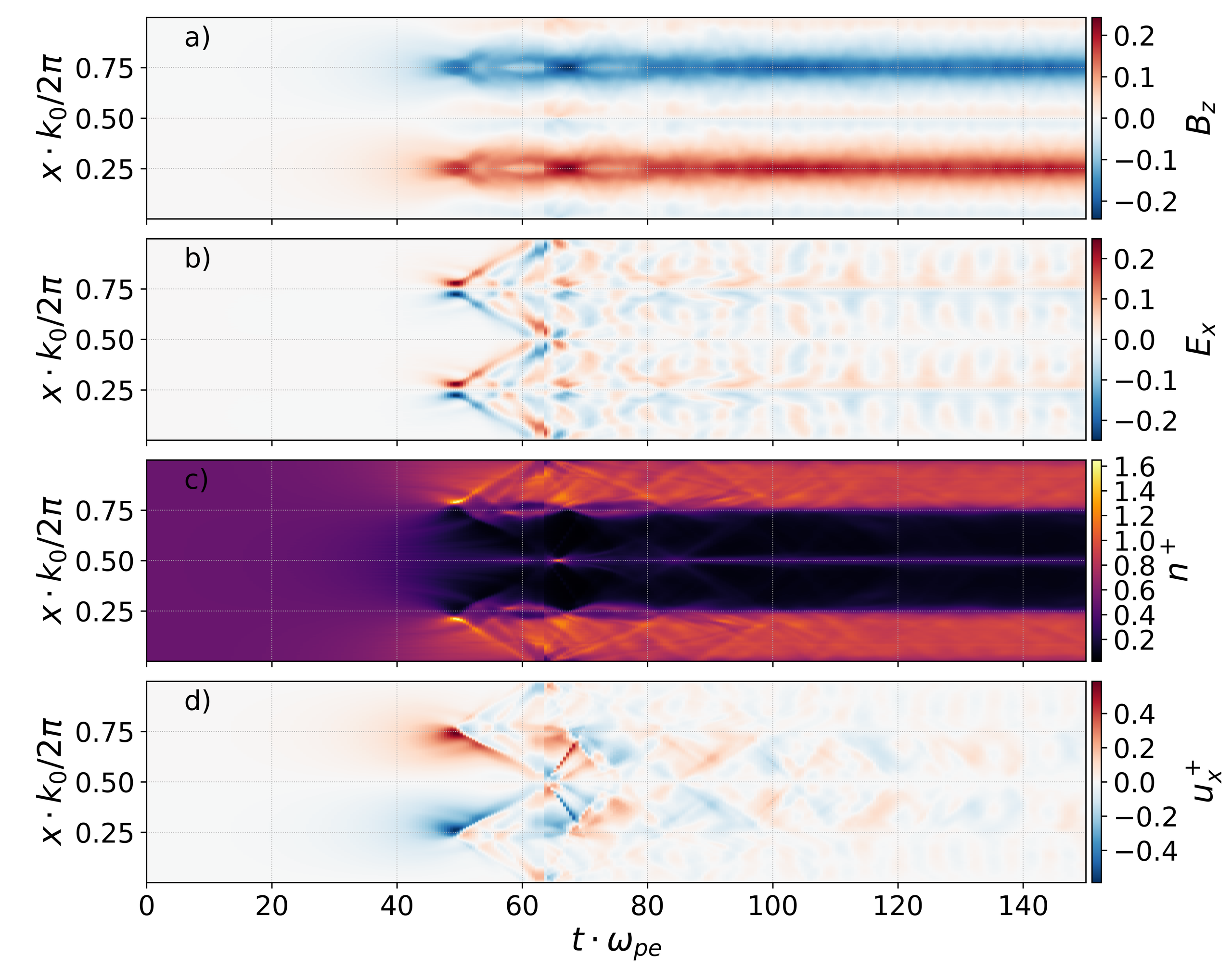

Figure 3: Evolution of field and plasma parameters in the low-temperature case.

The following figure shows the forces acting on the particle distributions and corresponding potential (defined as $\mathbf{F} = -\nabla\phi$). It is clear that for the low-temperature case, the electric field significantly alters the growth and saturation of the WI.

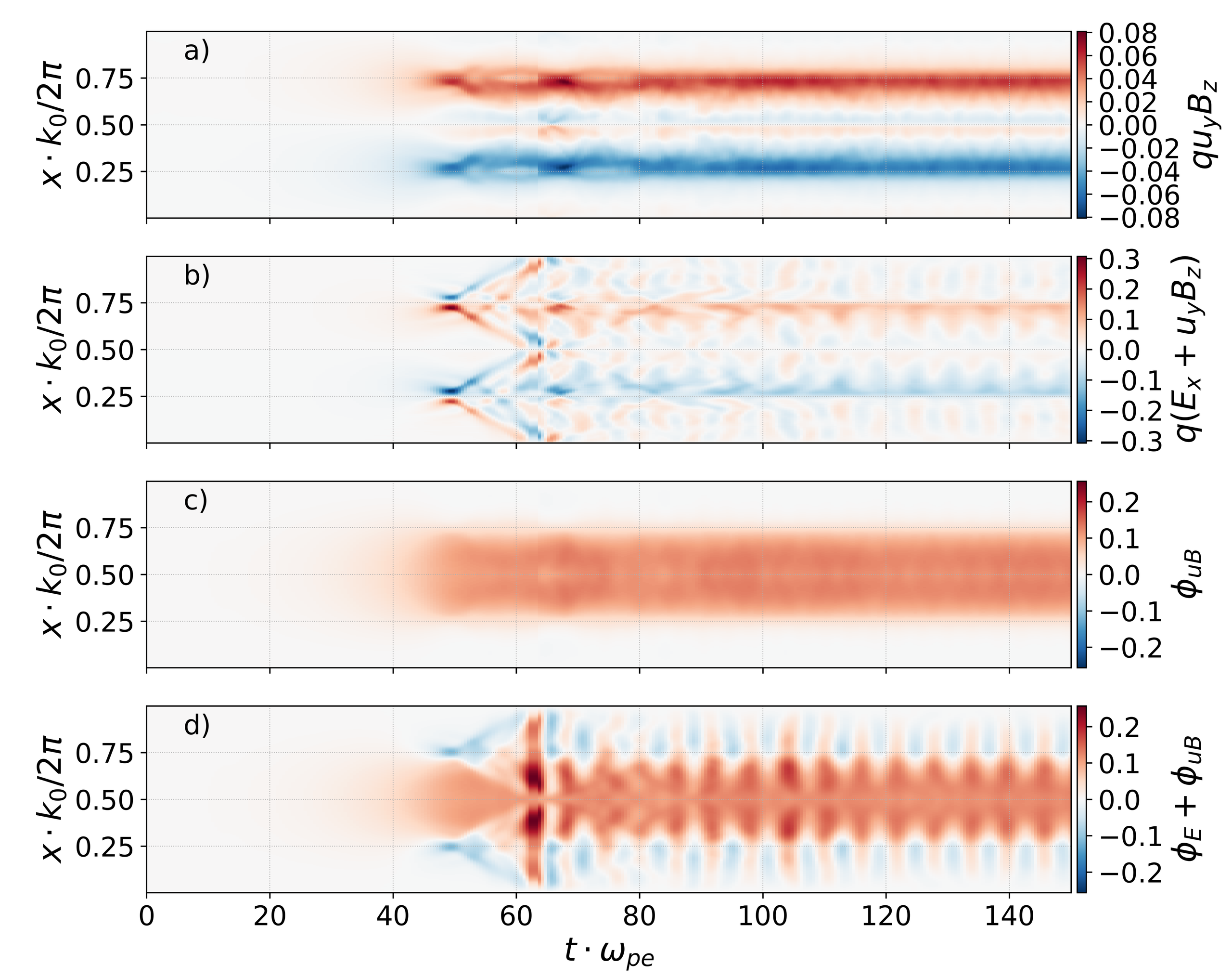

Figure 4: Evolution of the forces and corresponding potentials in the low-temperature case.

Phase-space Evolution

Following are plots of the particle distribution function at different times of the simulation. Since the distribution function is three dimensional (x, v_x, and v_y), the distribution function is integrated over one of the components in order to visualize it. Note the increase in the temperature (width of the distribution function).

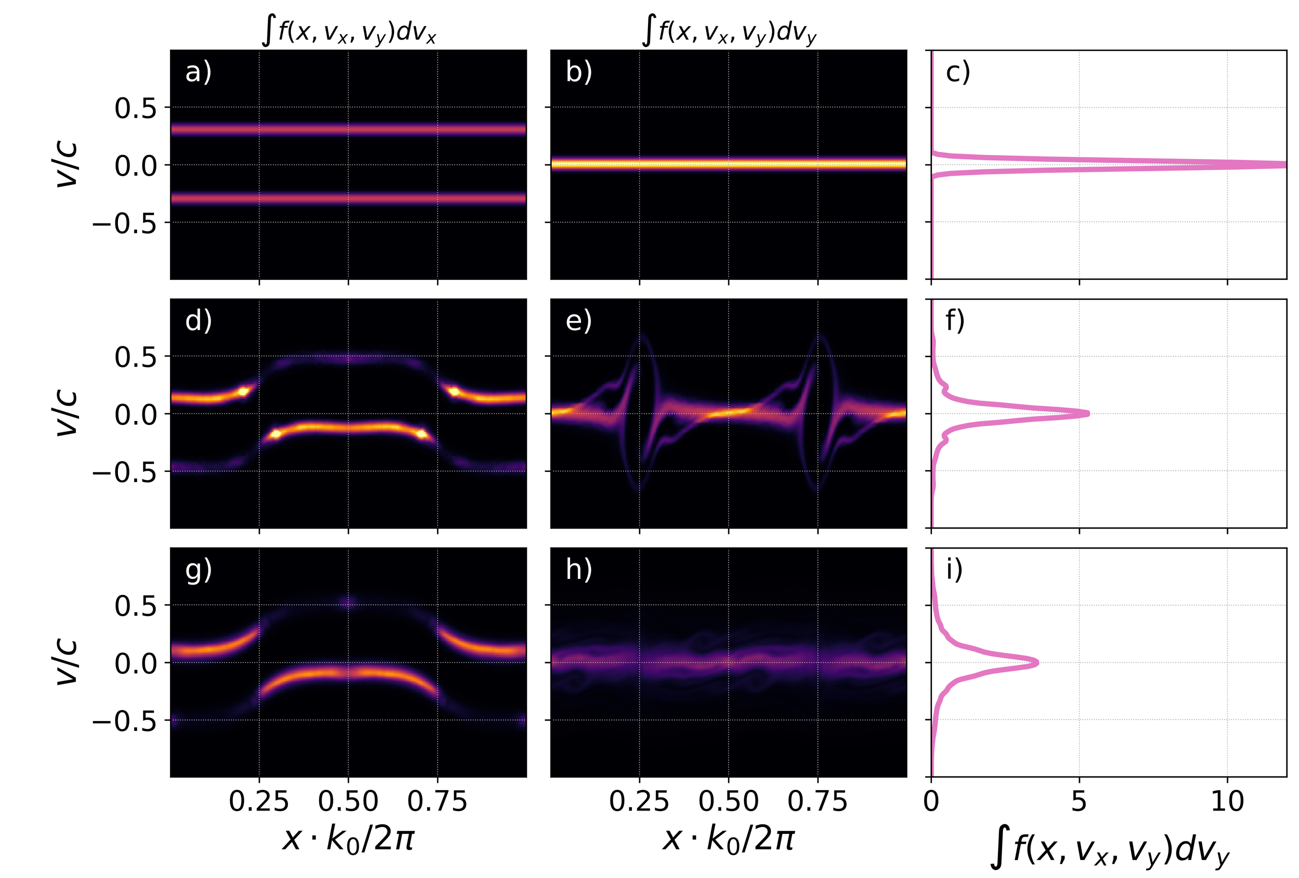

Figure 5: Phase-space plots of the particle distribution function for the low-temperature case. Plotted are initial conditions (top), state during the saturation (middle) and at the end of the simulation (bottom).

Summary

- The high-order continuum kinetic methods allow for noise-free interpretation of detailed plasma dynamics in the kinetic regime.
- Detailed description of plasma dynamics is presented leading to the nonlinear saturation of the WI with distribution functions described well into the nonlinear phase of the instability.
- Magnetic fields play a significant role in particle trapping; this agrees with previous work. The simulation results using $v_{th} = u_d$ confirm magnetic trapping as the sole mechanism of the instability saturation.
- However, for $v_{th} < u_d$, the role of electrostatic potential is also important. In the case of cold counter-streaming plasma beams, the electric field creates potential wells comparable to the magnetic field potential which significantly modifies the overall particle trapping.

Acknowledgments

This research was supported by the Air Force Office of Scientific Research under grant number FA9550-15-1-0193. The work of Ammar Hakim was supported by the U.S. Department of Energy under Contract No. DE-AC02-09CH11466.

The authors acknowledge Advanced Research Computing at Virginia Tech for providing computational resources and technical support that have contributed to the results reported within this paper. URL: http://www.arc.vt.edu

Reference

P. Cagas, A. Hakim, W. Scales, and Srinivasan B. Nonlinear saturation of the Weibel instability. *arXiv preprint arXiv:1705.07930*, 2017.

B. Cockburn and C. Shu. Runge-Kutta discontinuous Galerkin methods for convection-dominated problems. *Journal of scientific computing*, 16(3):173–261, 2001.

R. C. Davidson, D. A. Hammer, I. Haber, and C. E. Wagner. Nonlinear development of electromagnetic instabilities in anisotropic plasmas. *The Physics of Fluids*, 15(2):317–333, 1972.

J. Juno, A. Hakim, J. TenBarge, E. Shi, and W. Dorland. Discontinuous Galerkin algorithms for fully kinetic plasmas. *Journal of Computational Physics*, pages –, 2017. ISSN 0021-9991. doi: https://doi.org/10.1016/j.jcp.2017.10.009. URL http://www.sciencedirect.com/science/article/pii/S0021999117307477.